Fluid Dynamics of Airfoils with Moving Surface Boundary-Layer Control

F. Moktarian* and V. J. Modi†
University of British Columbia, Vancouver, Canada

Effectiveness of the moving surface boundary-layer control is assessed with reference to a symmetrical Joukowsky airfoil modified with a leading-edge rotating cylinder. Results of the test program and the numerical models suggest the following: 1) The surface singularity method is essential in modeling the complicated flow. With the inclusion of the boundary-layer correction scheme, it becomes an effective tool for obtaining useful information concerning moving surface boundary-layer control. The predicted pressure distributions are in good agreement with experiment almost up to the point of complete separation from the airfoil surface, except in the separation region, where the prediction of separated boundary layers with flow reversal would require the solution of the full Navier-Stokes equations. 2) The concept of moving surface boundary-layer control appears quite promising. The tests showed a significant improvement in maximum lift and stall characteristics. With cylinder rotation, the flow never separated completely from the upper surface for angles of attack as high as 48 deg. The higher rates of rotation ($U_c/U > 1$, U_c = cylinder surface velocity, U = freestream velocity) promoted reattachment of the partially separated flow, giving an increase in lift coefficient by as much as 150% for $U_c/U = 4$.

Introduction

EVER since the introduction of boundary-layer concept by Prandtl, there has been a constant challenge faced by scientists and engineers to minimize its adverse effects and control it to advantage. Methods such as suction, blowing, vortex generators, and turbulence promoters have been investigated at length and employed in practice with a varying degree of success. A vast body of literature accumulated over years has been reviewed rather effectively by several authors, including Goldstein,[4] Lachmann,[7] Rosenhead,[12] Schlichting,[14] Chang,[15] and others. However, the use of moving wall for boundary-layer control has received relatively less attention.

Irrespective of the method used, the main objective of a control procedure is to prevent or at least delay the separation of the boundary layer from the surface. A moving surface attempts to accomplish this in two ways: 1) it prevents the initial growth of the boundary layer by minimizing relative motion between the surface and the freestream, and 2) it injects momentum into the existing boundary layer.

Newton was probably the first to observe the effect of moving wall boundary-layer control on the trajectory of a spinning ball,[5] without any appreciation as to the basis of the effect. Almost 200 yrs later Magnus[1] studied lift generated by circulation and utilized the effect to construct a ship with a vertical rotating cylinder replacing the sail. Swanson[6] and Iverson[22] have presented excellent reviews of literature on the Magnus effect. As early as in 1910, Prandtl[8] himself demonstrated his "ship of zero resistance" through flow around two counterrotating cylinders, while Flettner[2] applied the principle to ship propulsion in 1924 when he fitted large vertical rotating cylinders on the deck of the "Buchau." A little later, in 1934, Goldstein[4] illustrated the principle of boundary-layer control using a rotating cylinder at the leading edge of a flat plate. However, the most practical application of moving wall for boundary-layer control was demonstrated by Favre.[3] Using an airfoil with upper surface formed by a belt moving over two rollers, he was able to delay separation until the angle of attack reached 55 deg, where the maximum lift coefficient of 3.5 was realized. Alvarez-Calderon and Arnold[9] carried out tests on a rotating cylinder flap to evolve a high-lift airfoil for STOL-type aircraft. The system was flight-tested on a single-engine high-wing research aircraft designed by the Aeronautics Division of the Universidad Nacional de Ingenieria in Lima, Peru.[11] Around the same time, Brooks[10] presented the preliminary results of his tests on a hydrofoil with a rotating cylinder at the leading edge or the trailing edge. For the leading-edge configuration, only a small increase in lift was observed; however, for the trailing-edge case, a substantial gain in lift resulted. Motivation for the test program was to assess improvement in fin performance for torpedo control. Along the same line, Steele and Harding[17] studied the application of rotating cylinders to improve ship maneuverability. From the overall consideration of hydrodynamic performance, mechanical complexity, and power consumption, a rotating cylinder at the leading edge of a rudder was preferred. Of some interest is the North American Rockwell OV-10A, which was flight-tested by NASA's Ames Research Center.[19,24,25] Cylinders located at the leading edges of the flaps are rotated at high speed with the flaps in lowered position. The main objective of the test program was to assess handling qualities of the propeller-powered STOL-type aircraft at higher lift coefficients. The aircraft was flown at speeds of 29-31 m/s along approaches up to -8 deg, which corresponded to the lift coefficient of about 4.3. In the pilot's opinion, any further reductions in approach velocity were limited by the stability and control characteristics. Excellent photographs of the airplane on ground (showing the cylinders in position) and in flight have been published in *Aviation Week and Space Technology*.[18]

Efforts so far, though useful to an extent, have been aimed generally at specific configurations and have lacked approach to the problem at a fundamental level in an organized fashion. From this point of view, Tennant's contribution to the field is significant. In 1971 Tennant presented an interesting analysis

Presented as Paper 86-2184 at the AIAA Atmospheric Flight Mechanics Conference, Williamsburg, VA, Aug. 18-20, 1986; received Aug. 20, 1986; revision received June 15, 1987.

*Graduate Research Assistant, Department of Mechanical Engineering.

†Professor, Department of Mechanical Engineering. Associate Fellow AIAA.

for the two-dimensional moving wall diffuser with a step change in area.[16,23] The diffuser incorporated rotating cylinders to form a part of its wall at the station of the area change. Preliminary experiments were also conducted for the area ratio up to 1:2.5, which showed no separation for appropriate moving surface to diffuser inlet velocity ratio. Tennant et al.[27] have also conducted tests with a wedge-shaped flap having a rotating cylinder as the leading edge. Flap deflection was limited to 15 deg, and the critical cylinder velocity necessary to suppress separation was determined. Effects of increase in gap size (between cylinder and flap surfaces) were also assessed. No effort was made to observe the influence of increase in cylinder speed beyond $U_c/U = 1.2$. More recently Tennant et al.[28] have reported circulation control for a symmetrical airfoil with a rotating cylinder forming its trailing edge. For zero angle of attack, the lift coefficient of 1.2 was attained with $U_c/U = 3$. Also of interest is their study concerning boundary-layer growth on moving surfaces accounting for gap effects.[29,32]

With reference to V/STOL application, the preliminary experimental study by Modi et al.[33] with NACA 63_3-218 airfoil used in the Canadair CL-84 must be mentioned. The experimental results suggested that the moving surface can provide quite effective boundary-layer control. It can lead to a significant increase in the maximum lift coefficient and stall angle. It appears that a rotating cylinder at the leading edge of an airfoil is likely to provide the maximum benefit.

Through a more recent study using analytical as well as numerical approaches, Mokhtarian and Modi concluded that the analytical potential-flow model can be used to obtain preliminary information concerning moving surface boundary-layer control. The information should be considered only qualitative in nature and indicative of trends. On the other hand, the numerical surface singularity procedure was found to be promising. It needed to be extended, however, to accommodate the corrections for the effects of wall confinement, viscosity, and flow separation.[34] The tests to prove the concept of moving surface boundary-layer control using a symmetrical Joukowsky airfoil modified with a leading-edge cylinder showed a significant improvement in maximum lift and stall characteristics.[35]

The investigation reported here builds upon this vast body of literature. It studies fluid dynamics of a Joukowsky airfoil with moving surface boundary-layer control using a numerical procedure consisting of:

1) A numerical surface singularity approach incorporating wall confinement and separated flow effects. This involves replacement of the airfoil and wind-tunnel wall surfaces with vorticity distribution in conjunction with appropriate constraint relations and inclusion of a source within the contour of the airfoil to model the wake when there is flow separation from the surface.
2) A finite-difference boundary-layer scheme to account for viscous corrections. This scheme uses potential-flow pressure distribution results to calculate the boundary-layer characteristics of the airfoil top and bottom surfaces starting at the stagnation point until the point of separation.
3) An iteration procedure that uses the boundary-layer displacement thicknesses calculated in the previous step to construct an equivalent airfoil by moving the airfoil surfaces in accordance with the local displacement thickness, and then iterates between the potential-flow method and the boundary-layer scheme to reach a final pressure distribution that no longer predicts separation from the airfoil surfaces.

The calculated pressure distribution and associated lift characteristics are substantiated through comparison with corresponding experimental results.

Numerical Surface Singularity Approach

A surface singularity, potential-flow model involving a distribution of vorticity on the airfoil surface and a boundary condition specified in terms of the stream function was used. The method, described in detail by Kennedy in his Ph.D. dissertation,[30] is thought to be the simplest available. Although the viscosity effects are ignored, it provides a fairly accurate estimate of the real flow around the section.

For flow over an airfoil section there can be no normal velocity at the solid surface; hence, it represents a streamline of the flow. The stream function is equal to a constant on the surface of the airfoil section. It consists of contributions from the uniform stream at an angle of attack α and distributed point vortices on the airfoil surface:

$$\Psi_{\text{constant}} = Y_s \cos\alpha - X_s \sin\alpha - \frac{1}{2\pi} \int_{S'} \gamma(S') \ln r(S,S')\, dS'$$

where an arbitrary point on the surface S is designated S'. The distances are nondimensionalized with respect to the chord length C, the velocities by U, and the stream functions using the product UC. The airfoil surface is divided into N small elements. On each of these there is a control point c_i located at (X_i, Y_i), where the given boundary condition is required to be satisfied. Each element j has a vorticity of density γ_j distributed on its surface. The integral over the whole surface is then replaced by a summation of N integrals over the N surface elements:

$$\Psi + \sum_{j=1}^{N} K_{ij}\, \gamma_j = Y_i \cos\alpha - X_i \sin\alpha \quad i = 1,\ldots, N$$

where Ψ is the stream function for the airfoil. K_{ij} is a coefficient representing the influence of element j on control point i. It is purely a function of the coordinates of the surface elements and the angle of attack. To satisfy the condition that the flow leaves the trailing edge smoothly (the Kutta condition), an extra control point is introduced a short distance downstream of the trailing edge. This generates an extra equation and therefore reduces the problem of potential flow over an airfoil section to that of solving $N + 1$ simultaneous equations. The velocity in the interior of the closed airfoil section is zero, and the discontinuity in tangential velocity across a vortex sheet is equal to the density of the vortex sheet. Thus, in solving the previous equations, one solves directly for the surface velocities on the airfoil components, γ_j.

The solution of the flow can easily be made to include one or more vortices at any location in the field. The stream function for a point vortex of known strength k (positive in the clockwise sense) located at (X_o, Y_o) is simply added to the right-hand side of the preceding equation:

$$\Psi + \sum_{j=1}^{N} K_{ij}\, \gamma_j = Y_i \cos\alpha - X_i \sin\alpha + \frac{k}{2\pi} \ell n\, r_i \quad i = 1,\ldots,$$

$$r_i = \sqrt{(X_i - X_o)^2 + (Y_i - Y_o)^2}$$

This method is extended to permit the analysis of airfoils with finite-thickness trailing edges. The vortex sheet defining the airfoil surface is open at the trailing edge in this case. A source singularity of unknown strength is now required within the contour of the body to model the flow inside the airfoil wake, which theoretically extends to infinity. Including the

stream function for the source in the previous equation gives

$$\Psi + \sum_{j=1}^{N} K_{ij}\,\gamma_j + \frac{m}{2\pi}\tan^{-1}\left(\frac{Y_i - Y_{\text{source}}}{X_i - X_{\text{source}}}\right) = Y_i\cos\alpha - X_i\sin\alpha + \frac{k}{2\pi}\ell n\, r_i \quad i = 1,\ldots,N$$

where m is the unknown source strength. The use of a second Kutta condition similar to the first one is now required to generate the extra equation needed to solve for the strength of the source. Since the velocity in the interior of the wing is not zero in this case, the local vortex sheet densities γ_j are no longer the surface velocities on the airfoil components. The tangential velocities, however, are contributions from the surface vorticity distribution as well as the uniform flow, the point source inside the contour, and the external vortex and can easily be calculated.

The preceding system of equations can be written in matrix form as

$$\begin{matrix} i=1 \\ i=N \end{matrix}\left(K_{ij}\right)\left(\gamma_j\right) + \left(S_i\right)m + \begin{pmatrix}1\\ \vdots \\ 1\end{pmatrix}\Psi = \left(R_i\right)$$

where R_i denotes the right-hand side of the stream function equation

$$R_i = Y_i\cos\alpha - X_i\sin\alpha + \frac{k}{2\pi}\ell n\, r_i$$

and

$$S_i = \frac{1}{2\pi}\tan^{-1}\left(\frac{Y_i - Y_{\text{source}}}{X_i - X_{\text{source}}}\right)$$

With the inclusion of the Kutta conditions, the system then becomes

$$\begin{matrix} i=1 \\ \\ i=N \\ i=N+1 \\ i=N+2 \end{matrix}\begin{bmatrix} K_{1,1} & \cdots & K_{1,N} & 1 & S_1 \\ \vdots & \ddots & \vdots & \vdots & \vdots \\ K_{N,1} & \cdots & K_{N,N} & 1 & S_N \\ \{\text{Kutta condition one}\} & & & 1 & S_{N+1} \\ \{\text{Kutta condition two}\} & & & 1 & S_{N+2} \end{bmatrix}\begin{bmatrix}\gamma_1 \\ \vdots \\ \gamma_N \\ \Psi \\ m\end{bmatrix} = \begin{bmatrix} R_1 \\ \vdots \\ R_N \\ R_{N+1} \\ R_{N+2}\end{bmatrix}$$

Extension of this method to the case of multicomponent configurations gives rise to a different stream function for each component, thus requiring corresponding Kutta conditions. It can also be applied to a configuration of an airfoil section between two walls, but the stream functions for the wall components have to be treated as known quantities since the flow rate between the walls is given. These known stream functions can thus be moved to the right-hand side of the equations and the unnecessary Kutta conditions removed. Also, the angle-of-attack modifications to the airfoil surface must be applied before the coefficient matrices are calculated, i.e., the airfoil must be rotated to the appropriate angle of incidence within the tunnel walls. In this case the system of equations can be written as

$$\begin{bmatrix} (K11)\begin{pmatrix}1\\ \vdots \\ 1\end{pmatrix}(S1)(K12)(K13) \\ \text{Kutta 1}\quad 1\quad S1_{N+1}\quad \text{Kutta 1}\quad \text{Kutta 1} \\ \text{Kutta 2}\quad 1\quad S1_{N+2}\quad \text{Kutta 2}\quad \text{Kutta 2} \\ (K21)\begin{pmatrix}0\\ \vdots \\ 0\end{pmatrix}(S2)(K22)(K23) \\ (K31)\begin{pmatrix}0\\ \vdots \\ 0\end{pmatrix}(S3)(K32)(K33) \end{bmatrix}\begin{bmatrix}(\gamma 1) \\ \Psi 1 \\ m \\ (\gamma 2) \\ (\gamma 3)\end{bmatrix} = \begin{bmatrix}(R1) \\ R1_{N+1} \\ R1_{N+2} \\ (R2-\Psi 2) \\ (R3-\Psi 3)\end{bmatrix}$$

Here $(K11)$ is the coefficient matrix calculated for the airfoil section, $(K22)$ and $(K33)$ are the coefficient matrices calculated for the wall components, and $(K12)$, $(K13)$, etc. represent the relations between the corresponding components. The system of equations is then solved by Gaussian elimination.

Viscous Corrections

In order to model the flow effectively over an airfoil section with boundary-layer control, however, effects of viscosity must be accounted for. These are confined to the boundary layer on the surface and to the separated-flow region near the trailing edge. The streamlines are shifted by a distance conventionally referred to as the "displacement thickness" of the boundary layer. The variation of the static pressure along the surface within the shear layer therefore depends on the shape of the surface and the displacement effect of the boundary layer. The flow outside this boundary layer is then approximated by the potential flow over the displacement surface.

A practical method of solving this problem is, therefore, to attempt to match the outer potential-flow solution with the inner boundary-layer solution. The thin shear-layer approximations of the Navier-Stokes equations for steady two-dimensional, incompressible flow are used. The thin shear-layer approximations for a boundary layer with negligible $\delta p/\delta y$ are

$$\frac{\delta u}{\delta x} + \frac{\delta v}{\delta y} = 0$$

$$u\frac{\delta u}{\delta x} + v\frac{\delta v}{\delta y} = -\frac{1}{\rho}\frac{dp}{dx} + (\nu + \epsilon)\frac{\delta^2 u}{\delta y^2}$$

along with the boundary conditions

$$y = 0, \qquad u = 0, \qquad v = 0$$

$$y \to \infty, \qquad u = U_e(x)$$

The pressure p is a known function of x, assumed independent of y, given by Bernoulli's equation along a streamline,

$$\frac{dp}{dx} = -\rho U_e \frac{dU_e}{dx}$$

and is input from the local potential-flow solution.

The finite-difference method used to solve the boundary-layer problem is that of Keller and Cebeci,[20,21] referred to as the "box" method. The system of equations is written in terms of a first-order system of PDE's using the standard Falkner-Skan transformation with the appropriate boundary conditions in terms of the transformed variables. The eddy viscosity term, $\epsilon^+ = \epsilon/\nu$, is expressed by the formulation explained by Cebeci and Smith,[26] which treats the turbulent boundary layer as a composite layer consisting of inner and outer regions with separate expressions for eddy viscosity in each region. The details of the formulation and the finite-difference procedure followed are those given by Cebeci and Bradshaw.[31]

Wind-Tunnel Test Program

For the wind-tunnel tests, a symmetrical Joukowsky model (15% maximum thickness-to-chord ratio), 0.38 m chord and 0.68 m long, modified with a leading-edge rotating cylinder, was constructed. Radius of the cylinder was so selected as to match average curvature of the leading edge. The details of the leading-edge geometry and the cylinder drive mechanism are shown in Fig. 1. The model spanned the tunnel test section, 0.91 × 0.68 × 2.6 m, to create an essentially two-dimensional condition. Primarily made of wood, the model carried a central aluminum pressure ring provided with 37 pressure taps suitably distributed over the circumference to yield detailed information concerning the surface loading. The model was supported by an Aerolab six-component strain gauge balance and tested in a low-speed return-type wind tunnel. The rectangular test section (0.91 × 0.68 m) was provided with 45-deg corner fillets varying from 15.25 × 15.25 to 12 × 12 cm to partly compensate for the boundary-layer growth.

The tests were carried out with a systematic variation of the angle of attack and cylinder rotational velocity. The pressure plots were integrated for each case to obtain lift coefficients. The lift was also measured independently using a strain gauge balance to substantiate the two-dimensional character of the test arrangement.

Numerical Results

A symmetrical Joukowsky airfoil was analyzed using the numerical surface singularity approach. The actual measured coordinates of the constructed experimental model, rather than the analytical shape, were input to the program to avoid problems due to differences between the "actual" and "ideal" sections. The ideal Joukowsky cusp character, e.g., is replaced with a finite-thickness trailing edge. Selected pressure-distribution and calculated-lift data are compared with the wind-tunnel results.

A typical pressure distribution as predicted by the potential flow model is shown in Fig. 2a. The model predicts slightly higher suction on the upper surface due to wall confinement. The correction scheme uses these results to calculate the displacement effect of the boundary layer as well as the point of separation before the final "corrected" pressure distribution can be obtained.

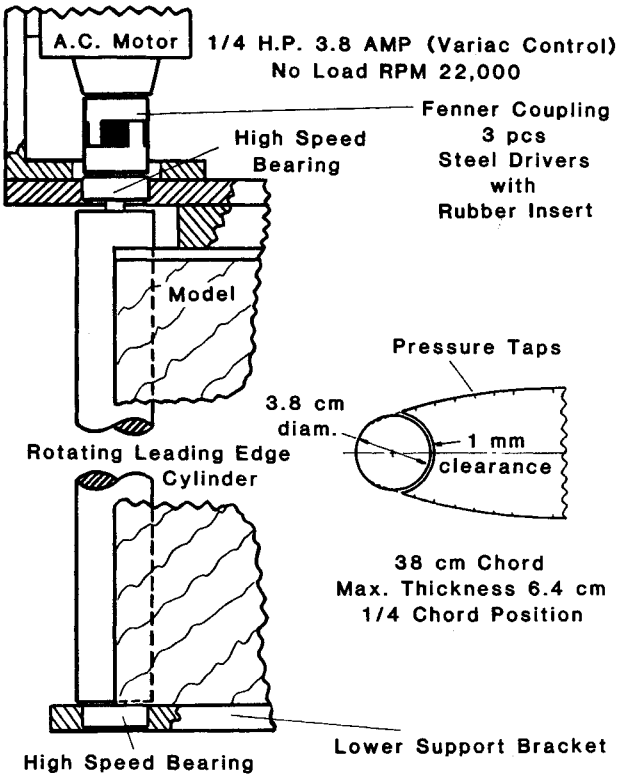

Fig. 1 Detailed schematic of the leading-edge rotating cylinder and cylinder drive mechanism.

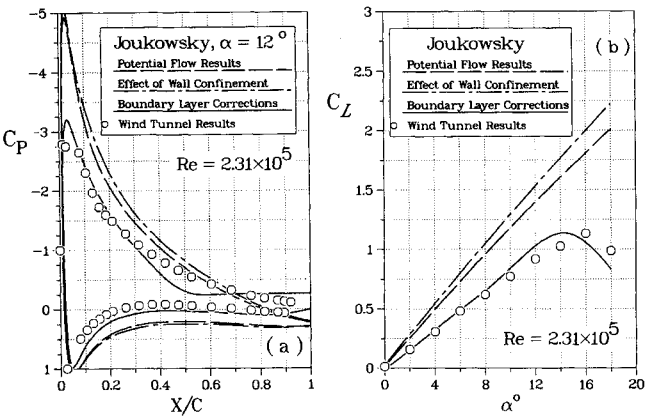

Fig. 2 Typical pressure distribution and calculated lift coefficients for a Joukowsky airfoil. Comparison between numerical results, corrected results, and experiment.

The disagreement between the predicted and experimental results at the trailing edge is believed to be mainly due to the nature of the boundary-layer scheme and its simplifying assumptions. Particularly, the assumption that the pressure is constant across the shear layer is no longer valid after the shear layer has separated and is only an approximation when the size of the separation region near the trailing edge of the airfoil is small. More accurate prediction of the pressure in a separated boundary layer with flow reversal would require the solution of the full Navier-Stokes equations. These results, along with the corresponding results at other angles of attack, are summarized in the form of coefficients of lift in Fig. 2b and highlight the improvements when the effect of the boundary layer is taken into account.

Next a Joukowsky airfoil with a rotating cylinder forming its nose is considered. A typical pressure distribution for this two-component airfoil, as predicted by the surface singularity method, is compared with experiment in Fig. 3a. Since the result of the cylinder rotation is in effect to minimize the

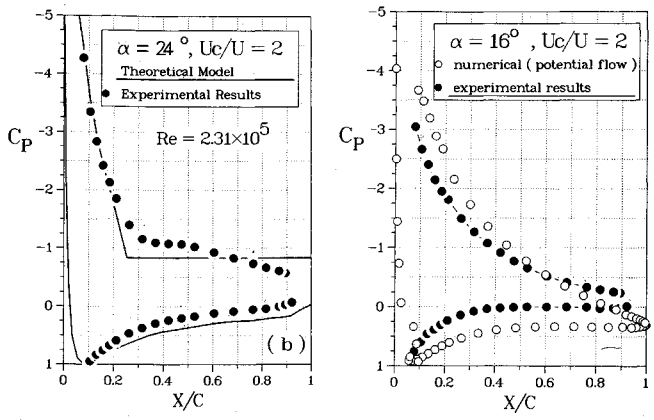

Fig. 3 Comparison between typical numerically and experimentally obtained pressure distributions on a Joukowsky airfoil.

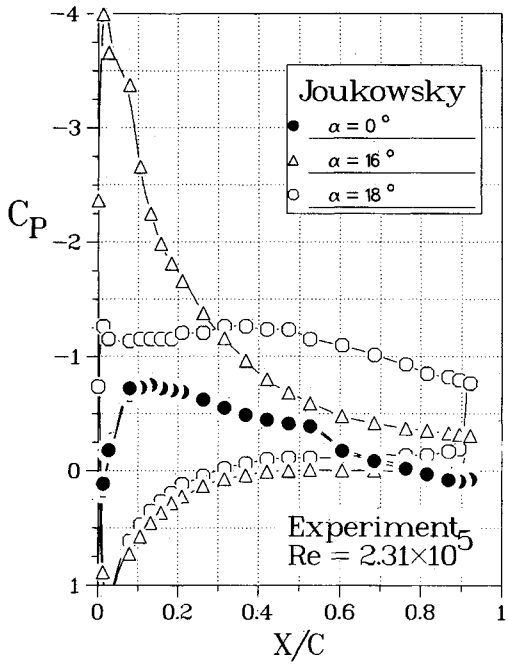

Fig. 4 Typical experimentally obtained pressure distribution plots for Joukowsky airfoil. This graph serves as reference to evaluate the effects of airfoil modifications and cylinder rotation.

adverse effects of the boundary layer, the correlation between the inviscid results and experiment remains reasonable.

At higher angles of attack, however, it is not possible to keep the flow attached over the entire upper surface. As the size of the separation region grows larger, the suction over the airfoil decreases and the correction of the inviscid results becomes essential. The pressure peak at the leading edge, predicted by the potential-flow solution, and the large adverse pressure gradient associated with it cause the boundary layer to separate immediately after the leading edge. Therefore, it is not even possible to apply the boundary-layer corrections unless the boundary-layer control scheme is also modeled.

The effect of the cylinder rotation is considered through the potential-flow model using a simple model of a pair of counterrotating vortices below the leading edge and through the boundary-layer scheme by setting the appropriate boundary conditions at the location of the leading-edge cylinder. Typical results are compared with the corresponding experimental results in Fig. 3b. The theoretical approach appears to be quite reasonable considering the very complicated nature of the flow. The location of the stagnation point on the lower surface and the separation point on the upper surface are predicted very accurately.

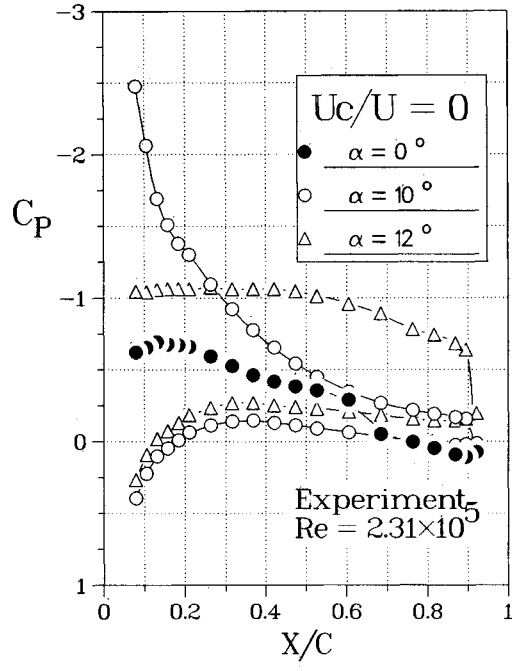

Fig. 5 Effect of modification of the Joukowsky airfoil with the leading-edge cylinder on the stall angle.

Wind-Tunnel Results

The symmetrical Joukowsky airfoil model (maximum thickness 15%) was tested systematically at a Reynolds number of 2.3×10^5 over a range of angles of attack and cylinder speeds ($U_c/U = 0, 1, 2, 3, 4$). The pressure plots were integrated for each case to obtain the lift coefficients. The amount of information obtained is rather extensive, however, and only a few of the typical results useful in establishing trends are recorded here.

Figure 4, which serves as a reference, shows pressure distribution on the surface of the Joukowsky airfoil model, without rotating cylinder replacing its nose. Thus, it represents pressure profiles for a conventional Joukowsky airfoil. Due to practical difficulty in locating pressure taps in the cusp region, there is an apparent discontinuity in the pressure plots near the trailing edge. However, that region has little importance in the present discussion. It is apparent that the airfoil stalls at an angle of attack somewhere between 16 and 18 deg.

Figure 5, which also serves as a reference, shows the adverse effect of replacing the nose by a nonrotating cylinder ($U_c/U = 0$). Again, the apparent discontinuity in the pressure plots near the leading edge is due to practical difficulty in the measurement of pressure at the surface of the cylinder. However, since in the subcritical flow regime the peak negative pressure on the surface of a circular cylinder occurs at around 70 deg, location of the first pressure tap (top and bottom surfaces) would come quite close to it. Note that only the nose geometry is slightly altered, however, now that we have a two-element airfoil with a gap in the form of a step from the cylinder surface to the airfoil surface. This sharp corner protruding into the thin boundary layer causes it to grow and separate much faster, therefore reducing the stall angle, which is now between 10 and 12 deg.

The pressure distribution plots before stall, however, do not show any significant deviation from the no-gap case except very close to the gap, where the presence of a sharp corner produces a slightly higher suction (Fig. 6). There seems to be little indication of any appreciable flow leakage from the bottom to the top surface through the cylinder airfoil interface, and the effect of the gap is, therefore, confined to causing stall at a lower angle in this case. It must be noted, however, that a large unsealed gap would allow communication of pressure between the high- and low-pressure regions

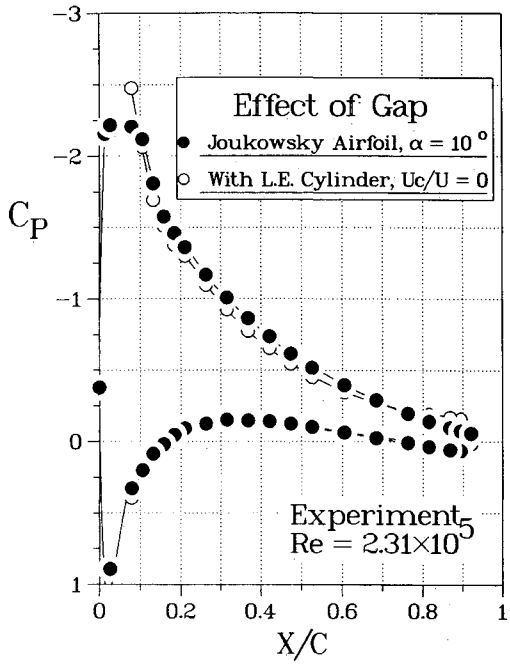

Fig. 6 Effect of the cylinder-airfoil gap on the pressure distribution of the Joukowsky airfoil at a given angle of attack.

and decrease the lift of the airfoil as well as the effectiveness of the cylinder.

Figure 7 shows the effect of cylinder rotation on the pressure distribution and the onset of stall. Four cases of $U_c/U = 1, 2, 3, 4$ are considered for which Fig. 5 serves as a reference. The plots bring to light several interesting points of information:

1) In general, the effect of the leading-edge rotating cylinder is to increase the peak negative pressure. However, the relative increase is less at higher U_c/U.

2) With an increase in cylinder surface velocity to freestream velocity ratio, the stall angle corresponding to complete separation (i.e., no reattachment) is delayed. Note that without rotation the separation (on the top surface) occurs at around 12 deg; however, with rotation, a part of the surface always has an attached flow up to $x/c \approx 0.25$.

3) Also, with high rates of rotation, the onset of flow separation on the top surface occurs at a higher angle of attack and there is a tendency for the boundary layer to reattach toward the trailing edge, as is evident in Fig. 7d.

4) One would, therefore, expect the overall effect of the cylinder to be increased ($C_{L,\max}$) due to stall at much higher angles of attack and higher C_L/C_D at any given angle of attack.

Figure 8 clearly shows the delay in stall brought about by the cylinder rotation. For $\alpha = 12$ deg, the airfoil has stalled in absence of the cylinder rotation. However, with $U_c/U = 2$ the flow reattaches, thus avoiding stall and the associated pressure collapse. Note, however, that at a sufficiently high angle of attack (say $\alpha = 32$ deg, Fig. 9), irrespective of the level of cylinder rotation, it is not possible to achieve completely attached flow over the top surface. Hence, the pressure distribution over the bottom surface remains essentially the same. Further increase in angle of attack only leads to an increase in the peak negative pressure at the leading edge.

The data for different rates of rotation of the cylinder are summarized in Fig. 10. The basic airfoil (without cylinder) has a maximum lift coefficient of around 1.1. However, bluffness of the cylinder and the associated gap cause earlier stall as well as diminished $C_{L,\max}$. In absence of the cylinder rotation the airfoil stalled at around 12 deg, giving uniform pressure distribution on the top surface. The stall was found to set in rather abruptly as shown by a sudden drop in lift. However,

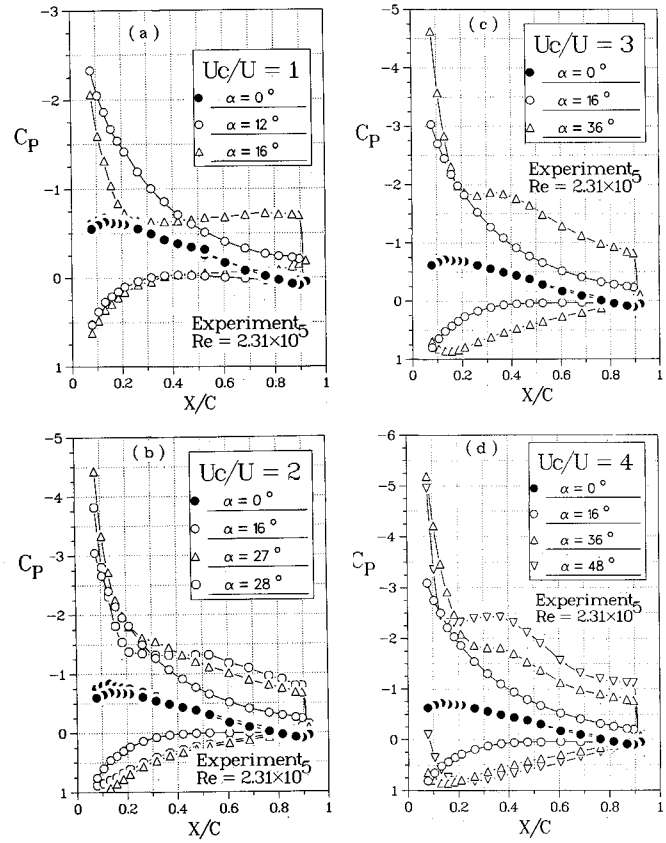

Fig. 7 Effects of cylinder rotation on the pressure distribution around a symmetrical Joukowsky airfoil: a) $U_c/U = 1$; b) $U_c/U = 2$; c) $U_c/U = 3$; and d) $U_c/U = 4$.

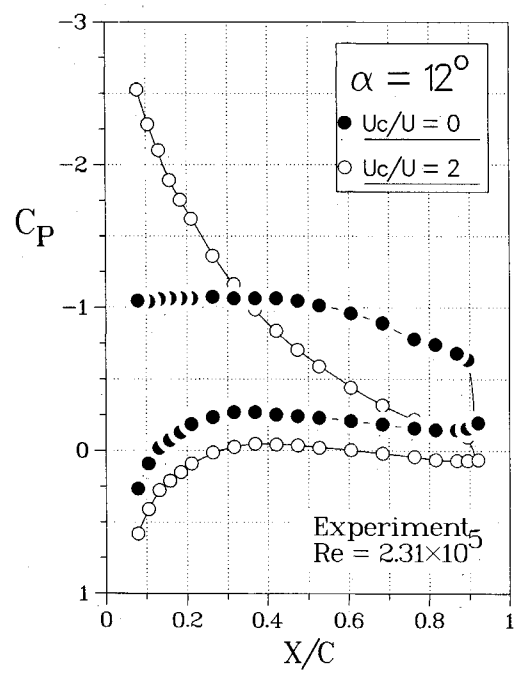

Fig. 8 Experimentally obtained pressure distribution plots showing the reattachment of the otherwise separated flow brought about by cylinder rotation.

with cylinder rotation a large, well-developed suction peak at the leading edge of the wing suggested a delay in the stall. In fact, the data showed the stall to occur around 32 deg ($U_c/U = 4$) with an increase in the lift coefficient by about 150%. Note also that the effect of rotation is to extend the lift curve without affecting its slope and flatten the stall peak.

Conclusions

Based on the numerical and experimental results, the following general conclusions can be made:

1) The numerical procedure appears to be quite reasonable, considering the very complicated nature of the flow, and is capable of predicting useful information concerning moving surface boundary-layer control.

2) Experimental results suggest that the concept of moving surface boundary-layer control is sound and effective. The availability of such a high value of lift from an analytical shape airfoil suggests that landing and takeoff speeds of a STOL-type airplane using this form of boundary-layer control could be drastically reduced.

Acknowledgment

The model was fabricated in the Mechanical Engineering workshop. The assistance of Mr. E. Abell, Senior Technician, in design and construction of the model is gratefully acknowledged. Investigation reported here was supported by the Natural Sciences and Engineering Research Council of Canada Grant A-2181.

References

[1]Magnus, G., "Ueber die Verdichtung der Gase an der Oberflache Glatter Korper," *Poggendorfs Annalen der Physik und Chemie,* Vol. 88, No. 1, 1853, pp. 604–610.

[2]Flettner, A., "The Flettner Rotor Ship," *Engineering,* Vol. 19, 1925, pp. 117–120.

[3]Favre, A., "Contribution a l'Etude Experimentale des Mouvements Hydrodynamiques a Deux Dimensions," Thesis presented to the University of Paris, 1938.

[4]Goldstein, S., *Modern Developments in Fluid Mechanics,* Vols. 1 and 2, Oxford University Press, 1938.

[5]Thwaites, B., *Incompressible Aerodynamics,* Clarendon Press, 1960, p. 215.

[6]Swanson, W.M., "The Magnus Effect: A Summary of Investigation to Date," Transactions of the ASME, *Journal of Basic Engineering,* Vol. 83, Sept. 1961, pp. 461–470.

[7]Lachmann, G.V., *Boundary Layer and Flow Control,* Vols. 1 and 2, Pergamon, 1961.

[8]Betz, A., "History of Boundary Layer Control in Germany," *Boundary Layer and Flow Control,* edited by G.V. Lachmann, Pergamon, Vol. 1, pp. 1–20.

[9]Alvarez-Calderon, A. and Arnold, F.R., "A Study of the Aerodynamic Characteristics of a High Lift Device Based on Rotating Cylinder Flap," Stanford University Technical Report RCF-1, 1961.

[10]Brooks, J.D., "Effect of a Rotating Cylinder at the Leading and Trailing Edges of a Hydrofoil," U.S. Naval Ordnance Test Station, Department of the Navy, NAVWEPS Rept. 8042, April 1963.

[11]Brown, D.A., "Peruvians Study Rotating-Cylinder Flap," *Aviation Week and Technology,* Vol. 88, No. 23, Dec. 1964, pp. 70–76.

[12]Rosenhead, L., *Laminar Boundary Layers,* Oxford University Press, 1966.

[13]"Report of the Research Coordination Group on Boundary Layer Control to Suppress Separation," Associate Committee on Aerodynamics, National Research Council, Sept. 1966.

[14]Schlichting, H., *Boundary Layer Theory,* McGraw-Hill, 1968.

[15]Chang, P.K., *Separation of Flow,* Pergamon, 1970.

[16]Tennant, J.S., "The Theory of Moving Wall Boundary Layer Control and its Experimental Application to Subsonic Diffusers," Ph.D. dissertation, Clemson University, May 1971.

[17]Steele, B.N. and Harding, M.H., "Applications of Rotating Cylinders for Ship Maneuvering," *Journal of Naval Architecture,* July 1971, pp. 27–29.

[18]"Rotating Cylinder Flaps Tested on OV-10A," *Aviation Week and Space Technology,* Vol. 95, No. 16, Oct. 1971, p. 19, and No. 24, Dec. 1971, cover page.

[19]Cichy, D.R., Harris, J.W., and MacKay, J.K., "Flight Tests of a Rotating Cylinder Flap on a North American Rockwell YOV-10A Aircraft," NASA CR-2135, Nov. 1972.

[20]Keller, H.B. and Cebeci, T., "Accurate Numerical Methods for Boundary-Layer Flows, Part 1, Two-Dimensional Laminar Flows," *Lecture Notes in Physics,* Vol. 8, *Proceedings of the Second International Conference on Numerical Methods in Fluid Dynamics,* Springer-Verlag, New York, 1971, p.92.

[21]Keller, H.B. and Cebeci, T., "Accurate Numerical Methods for Boundary-Layer Flows, Part 2, Two-Dimensional Turbulent Flows," *AIAA Journal,* Vol. 10, p. 1193, 1972.

[22]Iverson, J.D., "Correlation of Magnus Force Delta for Slender Spinning Cylinders," Paper 72-966, AIAA 2nd Atmospheric Flight Mechanics Conference, Palo Alto, CA, Sept. 11–13, 1972.

[23]Tennant, J.S., "A Subsonic Diffuser with Moving Walls for Boundary-Layer Control," *AIAA Journal,* Vol. 11, Feb. 1973, pp. 240–242.

[24]Weiberg, J.A., Giulianettij, D., Gambucci, B., and Innis, R.C., "Takeoff and Landing Performance and Noise Characteristics of a Deflected STOL Airplane with Interconnected Propellers and Rotating Cylinder Flaps," NASA TM X-62, 320, Dec. 1973.

[25]Cook, W.L., Mickey, D.M., and Quigley, H.G., "Aerodynamics of Jet Flap and Rotating Cylinder Flap STOL Concepts," AGARD Fluid Dynamics Panel on V/STOL Aerodynamics, Delft, Netherlands, April 1974, Paper No. 10.

[26]Cebeci, T. and Smith, A.M.O., *Analysis of Turbulent Boundary Layers,* Academic, New York, 1974.

[27]Johnson, W.S., Tennant, J.S., and Stamps, R.E., "Leading Edge Rotating Cylinder for Boundary-Layer Control on Lifting Surfaces," *Journal of Hydrodynautics,* Vol. 9, No. 2, April 1975, pp. 76–78.

[28]Tennant, J.S., Johnson, W.S., and Krothapalli, A., "Rotating Cylinder for Circulation Control on an Airfoil," *Journal of Hydronautics,* Vol. 11, July 1986, pp. 102–105.